NeuroImage 52 (2010) 549–555

Contents lists available at ScienceDirect

NeuroImage

journal homepage: www.elsevier.com/locate/ynimg

Real-time electrochemical monitoring of brain tissue oxygen: A surrogate for functional magnetic resonance imaging in rodents

John P. Lowry [a,*], Karen Griffin [a,1], Stephen B. McHugh [b], Andrew S. Lowe [c,2], Mark Tricklebank [d], Nicola R. Sibson [c]

[a] Department of Chemistry, National University of Ireland, Maynooth, Co. Kildare, Ireland
[b] Department of Experimental Psychology, University of Oxford, South Parks Road, Oxford, OX1 3UD, UK
[c] CR-UK/MRC Gray Institute for Radiation Oncology and Biology, University of Oxford, Radiobiology Research Institute, Churchill Hospital, Oxford OX3 7LJ, UK
[d] Centre for Cognitive Neuroscience, Eli Lilly and Co. Limited, Windlesham, Surrey, UK

ARTICLE INFO

Article history:
Received 15 January 2010
Revised 27 March 2010
Accepted 15 April 2010
Available online 21 April 2010

ABSTRACT

Long-term *in-vivo* electrochemistry (LIVE) enables real-time monitoring and measurement of brain metabolites. In this study we have simultaneously obtained blood oxygenation level dependent (BOLD) fMRI and amperometric tissue O_2 data from rat cerebral cortex, during both increases and decreases in inspired O_2 content. BOLD and tissue O_2 measurements demonstrated close correlation ($r = 0.7898$) during complete (0%) O_2 removal, with marked negative responses occurring *ca.* 30 s after the onset of O_2 removal. Conversely, when the inspired O_2 was increased (50, 70 and 100% O_2 for 1 min) similar positive rapid changes (*ca.* 15 s) in both the BOLD and tissue O_2 signals were observed. These findings demonstrate, for the first time, the practical feasibility of obtaining real-time metabolite information during fMRI acquisition, and that tissue O_2 concentration monitored using an O_2 sensor can serve as an index of changes in the magnitude of the BOLD response. As LIVE O_2 sensors can be used in awake animals performing specific behavioural tasks the technique provides a viable animal surrogate of human fMRI experimentation.

Introduction

Increases in neuronal activity are accompanied by changes in cerebral blood flow, blood volume and oxygenation that are collectively referred to as the hemodynamic response. Such changes form the basis of imaging techniques such as blood oxygenation level dependent (BOLD) functional magnetic resonance imaging (fMRI) (Bandettini et al., 1992; Ogawa et al., 1992). BOLD fMRI is a key tool in neuroscience because it provides a powerful non-invasive way of mapping the regional activity of the brain during the performance of sensory, motor or cognitive tasks. Image resolution to a few hundred micron also means that detailed structural and functional imaging data can be acquired in small laboratory animals (Houston et al., 2001; Jones et al., 2005; Preece, et al., 2001). However, motion constraints necessitate the use of anaesthetics in the majority of studies, thus limiting the functional processes that can be engaged whilst the animal is being scanned and potentially altering circuitry engagement.

The MRI signal intensity is sensitive to the amount of O_2 carried by haemoglobin: a change in the amount of O_2 carried by haemoglobin changes the degree to which haemoglobin disturbs a magnetic field (Westerink and Cremers, 2007). Thus, an increase in haemoglobin oxygenation compared to baseline results in an increased BOLD signal, and conversely greater deoxygenation leads to a negative BOLD response. Tissue O_2 is related to deoxyhaemoglobin through the oxygen-haemoglobin dissociation curve and the local O_2 concentration gradient. Using a dual microelectrode and Clark oxygen electrode, Thompson et al. (2003) made simultaneous co-localised extracellular measurements of tissue O_2 and neural activity in cat cerebral cortex and established a coupling between neural activity and oxidative metabolism. Later work has suggested that tissue O_2 concentration is more closely associated with synaptic activity and local field potentials than spiking events (Viswanathan and Freeman, 2007). However, data from imaging techniques remains difficult to interpret in terms of the underlying neuronal activity, largely because one of the principle factors influencing blood oxygenation, the cerebral metabolic rate of O_2 consumption ($CMRO_2$), is poorly understood. In particular, how neurometabolic changes vary temporally, spatially and in magnitude remains uncertain. Recent *in-vivo* studies using microelectrodes to measure cerebral tissue O_2 in real-time during sensory stimulation have begun to address these issues (Ances et al., 2001; Masamoto et al., 2003, 2008; Offenhauser et al., 2005). Results from such experiments can be compared with both optical and fMRI

* Corresponding author. Fax: +353 1 708 3815.
E-mail address: John.Lowry@nuim.ie (J.P. Lowry).
[1] Present address: UCD School of Medicine and Medical Science, Belfield, Dublin 4, Ireland.
[2] Present address: Experimental Neuroimaging Group, Old Road Campus Research Building, Roosevelt Drive, Oxford OX3 7DQ, UK.

1053-8119/$ – see front matter © 2010 Elsevier Inc. All rights reserved.
doi:10.1016/j.neuroimage.2010.04.187

imaging data in order to understand the important relationship between metabolic and haemodynamic changes associated with increases in neuronal activity (Bartlett et al., 2008). While such comparisons have yielded useful insights into these processes a significant limitation is that data are being compared across different experiments.

The aim of the current study, therefore, was to develop and validate techniques for the simultaneous measurement of fMRI responses and tissue O_2 concentration. We show here that this can be achieved in the rat by *in situ* long-term *in-vivo* electrochemistry (LIVE). LIVE focuses on the detection of substances in extracellular fluid (ECF) using electrochemistry with implanted amperometric sensors and biosensors. By implanting a microelectrode in a specific brain region, applying a suitable potential profile and recording the resulting Faradaic current, changes in the concentration of a variety of ECF species can be monitored. LIVE offers excellent spatial (~10 μm) and temporal (millisecond) resolutions, and a major advantage of long-term stability (continuous monitoring *in vivo* over several weeks) (Lowry and O'Neill, 2005; O'Neill, 1994; O'Neill et al., 1998; Stamford and Justice, 1996). This contrasts with measurements achieved by brain microdialysis which suffers from relatively large probe size (minimum ~200 μm), variable *in vivo* recovery which is dependent on flow rate and tissue stabilisation/probe fouling, the need to collect finite volumes of dialysates depending on the chosen detection method, and poor time resolution (1–10 min).

To achieve our aim, carbon fibre bundle electrodes were designed for O_2 monitoring, as carbon fibre has very weak paramagnetic properties compared to metal electrodes which can produce susceptibility artifacts and image degradation; we have previously used carbon fibre electrodes for electrical stimulation of the brain in fMRI studies in animals and demonstrated their compatibility with fMRI data acquisition (Austin et al., 2003, 2005). In order to mimic changes in O_2 utilisation and supply during neuronal activation we have changed the concentration of O_2 in the inspired air. While previous reports have calibrated the BOLD signal against CBF/$CMRO_2$ coupling using hypercapnia (Davis et al., 1998; Leontiev, et al., 2007), to our knowledge, this is the first report to show simultaneous recording and demonstrate direct correlation of BOLD and real-time tissue O_2 signal changes, thus laying the foundation for simultaneous measurement of metabolic and fMRI responses to neuronal activation. The long-term (months) *in-vivo* signal stability of the LIVE O_2 sensor (Bolger and Lowry, 2005) also means that the relationship of these changes to defined stimuli and behavioural response can be determined in an exactly parallel way to the use of fMRI in human neuropsychology.

Materials and methods

LIVE oxygen sensors

A wide variety of sensors have been used for direct monitoring of O_2 with the majority of measurements obtained using constant potential amperometry (CPA) at noble metal microelectrodes such gold (Cooper, 1963; El-Deab and Ohsaka, 2003; Holmström et al., 1998) or platinum (Clark et al., 1958; Hitchman, 1978; Travis and Clark, 1965; Ward et al., 2002). The use of carbon-based electrodes has been reported by several groups (Bazzu et al., 2009; Bolger and Lowry, 2005; Lowry and O'Neill, 1996; Venton et al., 2003) and they are often the electrode of choice because of their *in-vivo* stability and minimal surface poisoning (Bolger and Lowry, 2005). Reduction of O_2 at carbon electrodes is a two-electron processes producing H_2O_2:

$$O_2 + 2H^+ + 2e^- \rightarrow H_2O_2$$

$$H_2O_2 + 2H^+ + 2e^- \rightarrow 2H_2O$$

Since H_2O_2 is poorly oxidised at carbon irreversible electrochemical behaviour is observed (Taylor and Humffray, 1975; Zimmerman and Wightman, 1991). The rate-limiting step for this reduction is the initial one-electron step followed by protonation of the superoxide ion and further reduction (Taylor and Humffray, 1975).

Single thread Nafion®-coated carbon fibre cylinder electrodes (CFEs, diameter 5 μm), coupled with fast cyclic voltammetry, have previously been used for the measurement of dissolved O_2 in anaesthetised animals (Venton et al., 2003; Zimmerman and Wightman, 1991). However, the ideal sensor size for such *in vivo* applications should be at least equal to, or greater than, the dimension of the blood capillaries (~100 μm) in order to prevent direct blood sampling of dissolved O_2 (Bazzu et al., 2009; Bolger and Lowry, 2005; Lowry and O'Neill, 1996). The unmodified carbon fibre bundle electrodes used in this study were thus designed with a diameter of ~100 μm and were prepared by attaching carbon fibre threads (individual diameter ~10 μm, Goodfellow, Cambridge, UK) to Flexivolt® copper wire (Radionics, Northants, UK) using conductive silver epoxy (Chemtronics, Georgia, USA). Fibres were encased within a double-layered plastic insulating sheath. The carbon fibre bundle was exposed *ca.* 1.5 mm beyond the insulating sheath for insertion into the cortex. Although carbon fibre is a non-magnetic material, the conductive wire and silver epoxy can cause significant image artefacts if positioned close to the animals' head. To prevent this, the total length of the carbon fibre threads used was sufficiently long so that the connection point lay outside the RF coil once the animal was inside the probe.

Animal preparation

Male Sprague–Dawley rats (217 ± 19 g; $n = 3$) were anaesthetised with 2% isoflurane in 30% O_2:70% N_2O. The animals were positioned in a stereotaxic frame and the skull was exposed via a midline incision in the scalp. Three burr holes were drilled in the skull above the right hemisphere, and a recording CFE was positioned stereotaxically in the hindpaw motor cortex (1 mm posterior to Bregma, 3 mm lateral and at a depth of 1.5 mm). Via the remaining two burr holes, reference and auxiliary electrodes (CFEs) were positioned at the same depth in the same hemisphere anterior to the recording electrode (*ca.* 2.5 and 3.5 mm anterior to Bregma). The electrodes were initially fixed in position using superglue, and subsequently the exposed surface of the skull was covered in dental cement to secure the electrodes in position and seal the surface. The reference potential provided by the CFE in brain tissue was measured against a saturated calomel electrode (SCE) and found to be 23 ± 10 mV. Before experiments commenced, the recording potential (−900 mV) was applied to the working electrode (CFE sensor) for at least 30 min to allow the electrode to settle (stable background) *in situ*.

ECG electrodes were positioned subcutaneously for measurement of heart rate, and core body temperature was monitored and regulated at 37 ± 0.5 °C with a rectal probe and circulating warm water system. Isoflurane concentration was reduced to *ca.* 1.6% for the remainder of the experiment. In one animal the left femoral artery was cannulated for continuous blood pressure monitoring. Following surgery the animals were positioned in a home-built 50 mm i.d. quadrature volume resonator with integral stereotaxic frame.

fMRI

MRI measurements were performed on a horizontal bore 7 Tesla magnet with a Varian Inova spectrometer. For the fMRI experiments, a multi-echo gradient echo imaging sequence was used with the following parameters: flip angle = 20°; relaxation time (TR) = 27.3 ms; echo time (TE) = 7, 14, 21 ms (acquired within one TR); acquisition matrix = 192 × 64 (zero filled to 192 × 96); 1 slice, voxel size 0.47 mm × 0.47 mm × 1.5 mm; single average (dc offset corrected offline); 1.75 s per acquisition. A multi-echo acquisition improves the

sensitivity to BOLD contrast changes in areas affected by local macroscopic T2* artefacts (i.e. due to the carbon electrodes) by calculating the arithmetic mean of non-optimal shorter echo-times to increase statistical power (Lowe et al., 2002, 2007; Ireland et al., 2005). Slice position was 7 mm posterior to the rhinal fissure (1 mm posterior to Bregma), corresponding to the centre of the hindpaw motor cortex. For the O_2 removal (100% N_2O) experiments each fMRI run consisted of an initial baseline period of 102 images (*ca.* 3 min), followed by three blocks of 189 images during which O_2 was removed for the first 17 images (*ca.* 30 s) and followed by 5 min for baseline recovery. This protocol was repeated a minimum of twice in each animal. For the increased O_2 experiments each fMRI run consisted of an initial baseline period of 172 images (*ca.* 5 min), followed by three blocks of 206 images during which O_2 was increased for the first 34 images (*ca.* 1 min) and followed by 5 min for baseline recovery. This protocol was repeated a minimum of twice in each animal for 100% O_2 and once for 70% and 50% O_2 (two blocks from one of the 50% O_2 runs were lost due to technical problems).

In one animal, after all of the BOLD fMRI data sets had been acquired 0.15 ml of ferumoxtran-10 (12 mg Fe/kg; Sinerem®, Guerbet, France; gift from Guerbet Research) was injected intravenously for CBV fMRI measurements. This USPIO agent exhibits a long blood half-life (5–6 h in rat (Li and Freeman, 2007)), enabling CBV measurements to be made over a prolonged period following intravenous administration. CBV fMRI data sets were acquired using the same imaging paradigm as for the BOLD acquisition.

Following data acquisition, mean echo images were calculated from the arithmetic mean of the individual echo images. Subsequently, the brain was manually masked to remove extra-cranial signal and images were Gaussian smoothed with a kernel 2 times the in-plane resolution. Regions of interest (ROIs) were delineated on the images, either encompassing the hindpaw motor cortex for the O_2 removal experiments or the entire brain for the increased O_2 experiments (where signal changes were very small and assuming consistent global effects), and time-courses of signal response were obtained for each ROI from the mean echo data.

Electrochemical experiments in vitro

Experiments *in vitro* were carried out in a phosphate buffered saline (PBS) solution, pH 7.4: NaCl (BDH, AnalaR grade, 0.15 mol/L), NaH_2PO_4 (BDH, AnalaR grade, 0.04 mol/L), and NaOH (BDH, AnalaR grade, 0.04 mol/L) prepared using deoxygenated doubly distilled water. All experiments were performed in a standard three-electrode glass electrochemical cell containing 15 mL PBS at room temperature. For cyclic voltammetry experiments, where the applied potential is scanned at a fixed scan rate between defined potential limits, a saturated calomel electrode (SCE) was used as the reference electrode, and a Pt wire served as the auxiliary electrode. To attain effective deaeration, the PBS solution was vigorously purged with O_2-free N_2 (BOC Gases, average O_2 content 2 ppm, maximum O_2 content 5 ppm) for at least 30 min before recording began and a N_2 atmosphere maintained over the cell thereafter. In experiments involving solution O_2, either atmospheric air (from a RENA 101 or 102 air pump) or pure O_2 (compressed gas) was bubbled through the PBS for a similar period and the appropriate gaseous atmosphere maintained over the quiescent solution during recording of the currents.

For post *in-vivo* calibrations involving constant potential amperometry (CPA), where the detecting electrode is held at a constant potential sufficient to detect the oxidation or reduction of the target substance, the same three-electrode (sensor, reference and auxiliary) configuration of CFEs was maintained and the concentrations of solution O_2 taken as 0 μM (N_2-saturated), 200 μM (air saturated (Bourdillon et al., 1982; Zhang and Wilson, 1993)) and 1260 μM (O_2-saturated (Bourdillon et al., 1982)), respectively.

LIVE instrumentation and software

Cyclic voltammetry and CPA were carried out using a low-noise potentiostat (Biostat II, Electrochemical and Medical systems, Newbury, UK). Implanted electrodes were connected to the potentiostat through the Flexivolt® copper wire (Radionics), gold electrical contacts (Plastics One, Roanoke, VA, USA) and a screened six core cable (Plastics One). Data acquisition was performed with a notebook PC, a Powerlab/400 interface system (ADInstruments Ltd., Oxford, UK) and Chart for Windows (v 4.0.1) software (ADInstruments Ltd.). A low-pass digital filter (50 Hz cut-off) was used to eliminate mains AC noise and all data was recorded at 10 Hz.

All analysis was performed using Microsoft Excel and Prism (GraphPad Software Inc., CA, USA). The significance of differences observed was estimated using the Student's *t*-test for paired observations. Two-tailed levels of significance were used and $p<0.05$ was considered to be significant. All data are presented as mean ± S.E.M.

Results

LIVE O_2 signal characterisation and validation

In order to determine the position of O_2 reduction on the voltage axis of the carbon fibre cylinder electrodes (CFEs) cyclic voltammetry was performed. Characterisation voltammograms were recorded at 100 mV/s in N_2 (background) and air saturated PBS solutions. The potential chosen for CPA O_2 detection was −900 mV which is in the mass-transport limited region after the peak potential for O_2 reduction (*ca.* −800 mV).

In order to demonstrate that the LIVE CFE signal was sensitive to changes in tissue O_2 concentration *in vivo* with the animal inside the MRI radiofrequency (RF) coil the O_2 content of the inspired gases was either reduced (100% N_2O:0% O_2) for 30 s or increased (to 100%) for *ca.* 1 min to induce brief periods of hypoxia and hyperoxia respectively (Fig. 1). On decreasing the O_2 content the amperometric signal began to rapidly decrease after ca. 30 s, reaching a plateau and returning to baseline within 1 min of ceasing the O_2 decrease. Conversely, when the O_2 content was increased the current began to increase after a short delay (*ca.* 15 s) and continued to increase over the 1-min interval until the inspired O_2 was returned to the normal 70% N_2O:30% O_2. The O_2 levels then remained elevated for *ca.* 30 s before returning to baseline levels in a similar time interval to that observed for 100% N_2O.

Simultaneous LIVE O_2 and BOLD fMRI monitoring

Having demonstrated that changes in brain tissue O_2 could be monitored in real-time using LIVE with our CFEs and within the RF coil, experiments were then performed to simultaneously record LIVE and BOLD data. Following a baseline period of 3 min, the O_2 content of the inspired gases (70% N_2O:30% O_2) was either reduced (100% N_2O:0% O_2) for *ca.* 30 s or increased (to 50%, 70% or 100%) for *ca.* 1 min. This sequence was repeated several times (*n* values) in each animal for each condition. ECG was maintained between *ca.* 370 and 390 bpm and no significant effects of the alterations in inspired gases were detected in any of the animals. Similarly, in the one animal in which an arterial line was inserted, MABP was maintained at a constant level (105–115 mm Hg) throughout and no significant changes were observed on either decreasing or increasing inspired O_2 (Table 1). However, following complete O_2 removal a transient reduction in MABP occurred (maximum decrease 5.3 ± 0.3 mm Hg; $n=3$), which began approximately 10 s after restoration of 30% O_2 and had completely reversed within *ca.* 100 s.

Tissue O_2 and BOLD signals showed a marked negative response during the brief episodes (30 s, repeated several times (*n* values) in

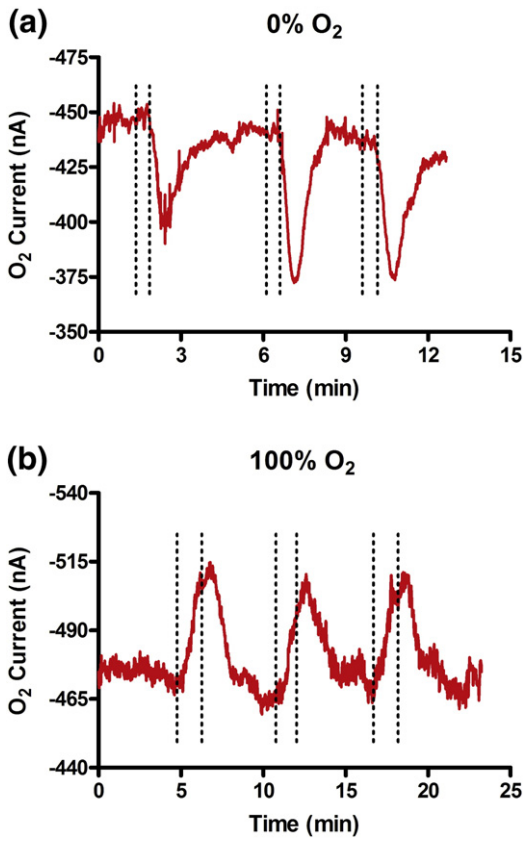

Fig. 1. Typical current-time responses recorded at an implanted carbon fibre electrode (CFE) for (a) successive 30 s decreases (100% N_2O: 0% O_2), and (b) 1 min increases (0% N_2O:100% O_2), in inspired O_2. CFE implanted in the motor cortex of a male Sprague-Dawley rat anaesthetised with 1.6% isoflurane in 70% N_2O:30% O_2. Hashed lines indicate periods of hypoxia and hyperoxia induced by changing the O_2 content of the inspired gases.

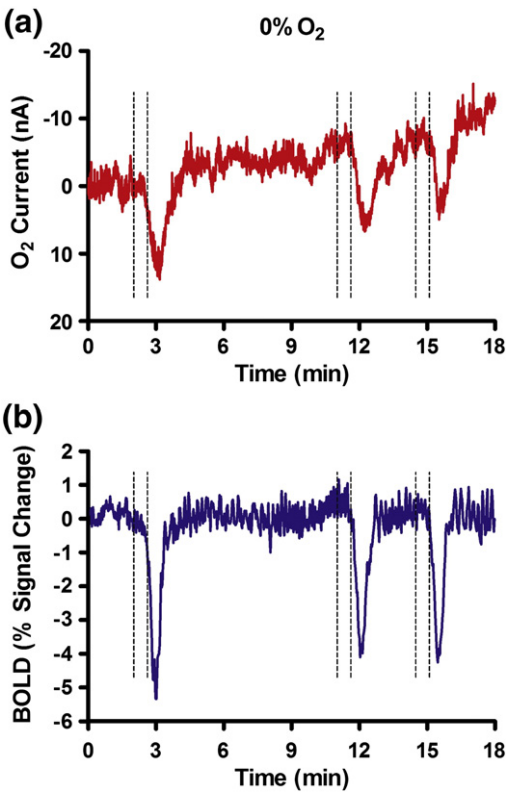

Fig. 2. Typical time courses for brain tissue O_2 (a) and BOLD fMRI (b) signals recorded simultaneously in response to successive 30 s periods (hashed lines) of decreased (100% N_2O:0% O_2) inspired O_2. BOLD data taken from ROI in region of recording CFE (hindpaw motor cortex). CFE background current subtracted from tissue O_2 signals.

each animal) of complete O_2 removal (Fig. 2), which will both increase deoxyhaemoglobin levels and decrease tissue O_2. The average O_2 current recorded using CPA decreased by 37.4 ± 8.3 nA ($n = 10$, $p < 0.0015$) below baseline (-490.0 ± 57.8 nA). Because of the high baseline currents observed *in vivo* it is not possible to calculate a percentage change in O_2 levels from the *in vivo* signal (Lowry et al., 1997). However, post *in vivo* calibrations of the CFEs indicate that the sensitivity for O_2 is -287.6 ± 78.3 nA/mM ($n = 3$). Therefore, using these calibrations the decrease in O_2 observed corresponds to an approximate change in concentration of 129.9 ± 28.6 μM, $n = 10$. The BOLD signal decrease and return to baseline followed the same time course as that of tissue O_2 with a maximum decrease of $6.6 \pm 1.5\%$ ($n = 10$) below baseline. A correlation analysis (Δ BOLD *vs.* Δ Current) indicates a significant correlation between the changes observed in the two signals ($r = 0.7898$, $p < 0.007$).

Conversely, when the inspired O_2 was increased positive changes in both the tissue O_2 and BOLD signals were observed (Fig. 3). The average O_2 current increased from a baseline of -323.8 ± 20.7 nA ($n = 36$) to a maximum of 16.61 ± 3.97 nA ($n = 9$, $p < 0.004$) for 50% O_2, 20.72 ± 3.76 nA ($n = 9$, $p < 0.0006$) for 70% O_2, and 32.80 ± 4.65 nA ($n = 18$, $p < 0.0001$) for 100% O_2 ($r^2 = 0.974$). Using post *in vivo* calibrations the increases in O_2 observed correspond to approximate changes in concentration of 57.69 ± 13.77 μM, (50% O_2, $n = 9$), 71.95 ± 12.75 μM, (70% O_2, $n = 9$) and 113.90 ± 16.13 μM, (100% O_2, $n = 18$) respectively. The BOLD signal increased and returned to baseline following the same time course as that of tissue O_2 with a maximum increase above baseline of $0.67 \pm 0.09\%$ ($n = 9$) for 50% O_2, $0.84 \pm 0.08\%$ ($n = 9$) for 70% O_2, and $1.07 \pm 0.09\%$ ($n = 18$) for 100% O_2 ($r^2 = 0.999$).

Table 1
Effect of O2 challenges on MABP. No significant differences were found between baseline recordings and those obtained during alteration of inspired O2 concentration: 100% O2 (each period is the average of two separate runs), 70%, 50% and 0% O2 (data from a single run).

	MABP (mm Hg)							
	100% Oxygen		70% Oxygen		50% Oxygen		0% Oxygen	
	Mean	S.E.M.	Mean	S.E.M.	Mean	S.E.M.	Mean	S.E.M.
Baseline #1	111.2	0.1	106.4	0.0	109.0	0.0	105.3	0.2
Oxygen #1	111.2	0.3	106.6	0.1	108.1	0.1	102.3	0.0
Baseline #2	111.7	0.1	108.3	0.1	107.2	0.0	104.0	0.3
Oxygen #2	111.5	0.2	108.1	0.1	106.9	0.1	103.2	0.0
Baseline #3	111.8	0.1	108.6	0.0	107.4	0.1	102.9	0.2
Oxygen #3	111.9	0.3	107.9	0.1	108.0	0.1	103.6	0.1
Baseline #4	112.3	0.2	110.9	0.3	106.3	0.0	102.8	0.1

Simultaneous LIVE O_2 and CBV fMRI Monitoring

In order to investigate the role of vasodilatory haemodynamics simultaneous LIVE and CBV fMRI was performed during the 100% O_2 paradigm. The CBV fMRI measurements were obtained using a long half-life iron oxide contrast agent (ferumoxtran-10; Sinerem®, Guerbet, France) to label the blood pool (Mandeville et al., 2004). A moderate increase (*ca.* 4%) in the CBV fMRI signal, indicating a *reduction* in USPIO concentration and hence blood volume in the brain, was observed during the periods of 100% O_2 (Fig. 4; CBV signals have been inverted to illustrate the reduction in CBV). Positive changes in the tissue O_2 signal were observed as before.

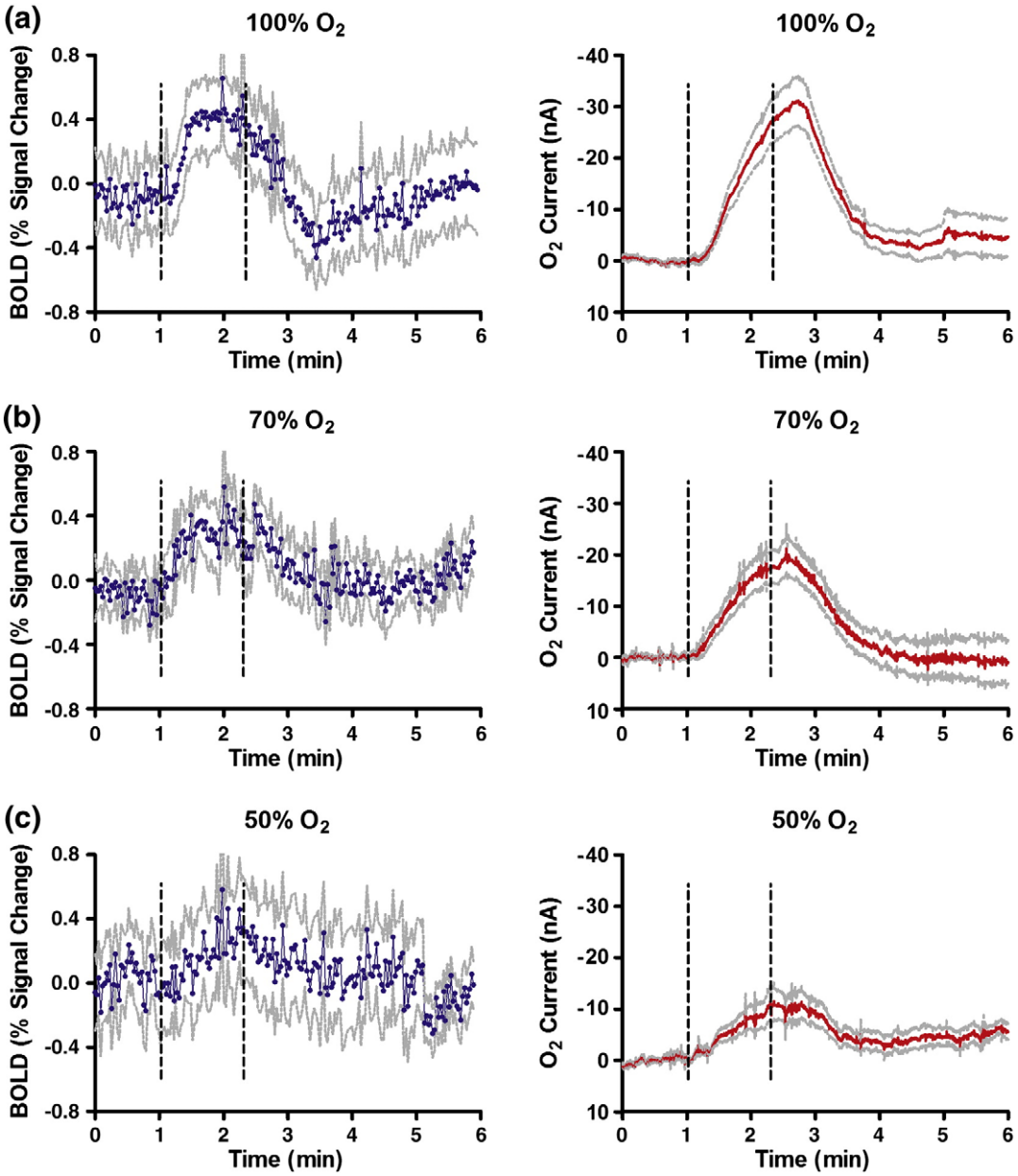

Fig. 3. Averaged time courses (Mean ± SEM) for BOLD fMRI (left) and brain tissue O_2 (right) signals recorded simultaneously in response to successive *ca.* 1 min periods (hashed lines) of increased inspired O_2: (a, $n=7$) 0% N_2O:100% O_2; (b, $n=9$) 30% N_2O:70% O_2; (c, $n=18$) 50% N_2O:50% O_2. BOLD data taken from ROI encompassing whole brain (1.5 mm thick imaging slice) and CFE background current subtracted from tissue O_2 signals.

Discussion

In this study we have developed and validated techniques for simultaneous measurement of fMRI responses and tissue O_2 concentration *via* LIVE. The results presented demonstrate the practical feasibility of obtaining real-time information about O_2 delivery and utilisation during fMRI acquisition. In the experiments described here, we have artificially decreased or increased blood and tissue O_2 content through variation of inspired gases and shown correlation between the fMRI and LIVE signals. The BOLD signal is based on a combination of local changes in deoxyhaemoglobin content, cerebral blood volume (CBV) and regional cerebral blood flow (CBF). Under the current experimental conditions the changes observed are likely to reflect mainly changes in deoxyhaemoglobin levels, although there may also be associated changes in CBF and CBV. Thus, during complete O_2 removal, deoxyhaemoglobin levels will increase markedly throughout the circulation and this in itself will give rise to a decrease in both fMRI and LIVE O_2 signals. However, there may also be a compensatory increase in CBF and/or CBV as part of the autoregulatory response. During the period of O_2 removal this increase in cerebral perfusion is expected to have relatively little effect on the fMRI signals as the blood is likely to be completely deoxygenated already and increased flow rate will not decrease the signal further. It is possible that increased cerebral perfusion may potentiate the O_2 signal decrease by causing O_2 to be removed from the brain tissue (reversal of normal O_2 gradients). However, given the short period of O_2 removal, it is perhaps more likely that increased perfusion contributes to the very rapid return to baseline values once O_2 is returned to the inspired gases.

It is generally assumed that haemoglobin is fully oxygenated on leaving the lungs under normal (30% O_2) conditions (Hsia, 1998), however it is possible that under anaesthesia this is not the case

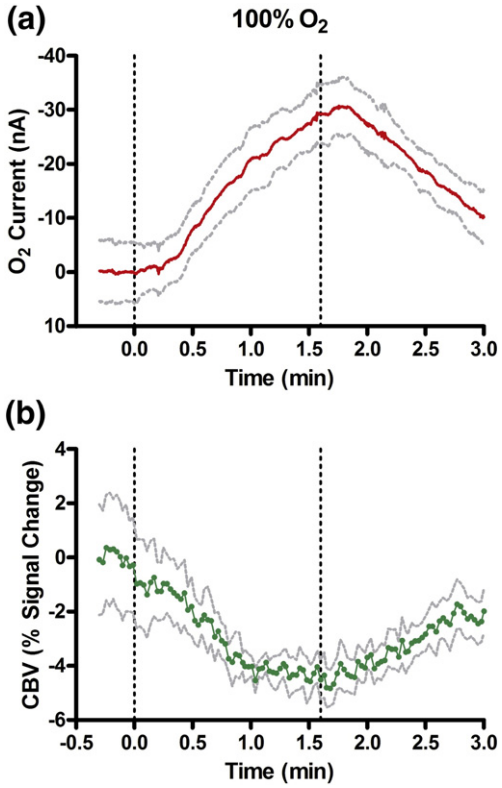

Fig. 4. Averaged time courses (Mean ± SEM) for brain tissue O_2 (a) and CBV fMRI (b) signals recorded simultaneously in response to *ca.* 1 min period (hashed lines) of 100% inspired O_2 ($n = 4$). CBV data taken from ROI encompassing whole brain (1.5 mm thick imaging slice) and have been inverted for ease of interpretation, since a positive change in the CBV signal (as measured) reflects a decrease in CBV. CFE background current subtracted from tissue O_2 signals.

(Seagard et al., 1985). Thus, when inspired O_2 is increased, the observed effects may arise through a combination of increased haemoglobin oxygenation (i.e. reduced deoxyhaemoglobin in the brain) and an increase in the amount of dissolved O_2 in the blood. The latter would be expected to have the effect of increasing tissue O_2 concentration (and hence LIVE O_2 signal) and also decreasing the rate of haemoglobin deoxygenation as it passes through the brain (and hence fMRI BOLD signal). Interestingly, molecular O_2 has a weak paramagnetic effect (Tadamura et al., 1997) which would reduce the BOLD signal, and thus the observed effects may be a balance of the two opposing influences. It has been shown previously that a transient increase in inspired O_2 does not cause an increase in CBF (Lowry et al., 1998), and it is unlikely, therefore, that the observed BOLD changes can be explained by a vasodilatory haemodynamic effect.

To investigate this, in one animal we also obtained simultaneous LIVE and CBV fMRI measurements during 100% O_2 administration. Since a reduction in CBV would not be expected to result in an increased BOLD signal (as measured under the same conditions), the effect of the observed decrease in CBV must again be smaller than the effects of increased pO_2 in the blood on the oxygenation level of haemoglobin. The decrease in CBV suggests a vasoconstrictory effect of hyperoxia, which is in agreement with very recent work from MacVicar's group, who showed that levels of prostaglandin E_2 (PGE_2) are modulated by extracellular levels of lactate and, thus, in turn tissue pO_2 (Gordon et al., 2008). PGE_2 produced in astrocytes via the arachidonic acid pathway has recently gained much support as a key mediator of vasodilation in the brain (for review see Iadecola and Nedergaard, 2007). Consequently, Gordon et al. (2008) suggest that steady-state CBF may be altered by levels of tissue pO_2 (and lactate) as a result of astrocytic regulation and modulation of PGE_2 levels. Thus, under hyperoxic conditions, tissue O_2 is high and lactate will be low, leading to a reduction in PGE_2 release and, consequently, vasoconstriction. This hypothesis has only been tested in *ex vivo* preparations to date, whilst the current data provide preliminary *in vivo* support and suggest that our combined LIVE/fMRI approach may provide a sensitive *in vivo* means to further investigate this concept.

Whatever the underlying causes are for the global changes in tissue oxygenation observed, it is clear that in both experimental conditions the BOLD signal, which reflects the local concentration of deoxyhaemoglobin, provides a close correlate of the tissue O_2 dynamics, or, alternatively, that tissue O_2 concentration can serve as an index of changes in the magnitude of the BOLD response. We have previously shown that LIVE measurements of tissue O_2 are closely related to CBF (Lowry et al., 1997), and it has been assumed, but not proven, that BOLD fMRI signals induced during neuronal activity reflect tissue O_2 levels (Dousset et al., 1999; Thompson et al., 2003, 2004, 2005; Raichle, 1998). The findings of this study now provide strong evidence to support this assumption and demonstrate that this novel combined technology provides a means of interrogating the relationships between metabolism, haemodynamics and neuronal activity. Moreover, our findings provide support for the use of LIVE to predict the BOLD response under conditions that are not amenable to the magnet environment, such as in awake rats performing specific behavioural tasks. Preliminary data indicate that LIVE measurements of tissue O_2 in the amygdala during extinction of fear conditioning (Li et al., 2009), in the nucleus accumbens during anticipated reward (Gilmour et al., 2009), and in the medial prefrontal cortex and nucleus accumbens following administration of glutamatergic psychostimulants (Ishiwari et al., 2009), are consistent with changes in the BOLD response seen in equivalent brain regions of human volunteers undergoing similar manipulations. Given that fMRI enables one to define the entire brain 3-dimensional pattern of neuronal activity, and BOLD fMRI specifically permits high resolution capture of O_2 levels throughout the brain, LIVE cannot substitute for either of these methodologies in terms of providing whole brain information. However, with the possibility of implanting several electrodes at any one time the measurement of the synchrony of activity with high temporal resolution between brain regions is a realistic possibility. In addition, LIVE technology can be applied to the measurement of many different neurochemicals, both metabolic and neuronal. Thus this combined methodology opens up numerous avenues for investigating the direct relationship between fMRI signal changes and the underlying neurochemistry across a range of different stimulation paradigms. Future work will concentrate on investigating the relationship between BOLD and tissue O_2 when variations in metabolic demand are induced by local stimulation.

Conclusion

The presented results indicate that the BOLD signal, which reflects the local concentration of deoxyhaemoglobin, provides a close correlate of tissue O_2 dynamics. These findings support the use of LIVE monitoring of tissue O_2 concentration as an index of changes in the BOLD response under conditions that are not amenable to the magnet environment, such as in conscious rodents performing specific behavioural tasks. Whilst local field potentials and/or single unit activity can be monitored in behaving animals, measurement of the biochemical parameters underlying fMRI offers a directly translational approach to the study of brain activity underlying function. The simultaneous acquisition of tissue O_2 concentration and fMRI data represents a significant step forward in modern neuroscience as it provides a viable awake animal surrogate of human fMRI experimentation, and thus is an effective translational tool which can better enable the comparison of human and animal research.

Acknowledgments

The authors gratefully acknowledge the suggestions and advice of Dr. Marianne Fillenz, Dr. David Bannerman (University of Oxford) and Dr. Jeffrey Glennon (formerly NUIM).

References

Ances, B.M., Buerk, D.G., Greenberg, J.H., Detre, J.A., 2001. Temporal dynamics of the partial pressure of brain tissue oxygen during functional forepaw stimulation in rats. Neurosci. Lett. 306, 106–110.

Austin, V.C., Blamire, A.M., Allers, K.A., Sharp, T., Styles, P., Matthews, P.M., Sibson, N.R., 2003. Differences in the BOLD fMRI response to direct and indirect cortical stimulation in the rat. Magn. Reson. Med. 49, 838–847.

Austin, V.C., Blamire, A.M., Allers, K.A., Sharp, T., Styles, P., Matthews, P.M., Sibson, N.R., 2005. Confounding effects of anesthesia on functional activation in rodent brain: a study of halothane and alpha-chloralose anesthesia. Neuroimage 24, 92–100.

Bandettini, P.A., Wong, E.C., Hincks, P.S., Tikofsky, R.S., Hyde, J.S., 1992. Time course EPI of human brain function during task activation. Magn. Reson. Med. 25, 390–397.

Bartlett, K., Saka, M., Jones, M., 2008. Polarographic electrode measures of cerebral tissue oxygenation: implications for functional brain imaging. Sensors 8, 7649–7670.

Bazzu, G., Puggioni, G., Dedola, S., Calia, G., Rocchitta, G., Migheli, R., Desole, M.S., Lowry, J.P., O'Neill, R.D., Serra, P.A., 2009. Real-time monitoring of brain tissue oxygen using a miniaturized biotelemetric device implanted in freely moving rats. Anal. Chem. 380, 323–330.

Bolger, F.B., Lowry, J.P., 2005. Brain tissue oxygen: in vivo monitoring using carbon paste electrodes. Sensors 5, 473–487.

Bourdillon, C., Thomas, V., Thomas, D., 1982. Electrochemical study of D-glucose oxidase autoinactivation. Enzyme Microb. Technol. 4, 175–180.

Clark Jr., L.C., Misrahy, G., Fox, R.P., 1958. Chronically implanted polarographic electrodes. J. Appl. Physiol. 13, 85–91.

Cooper, R., 1963. Local changes of intra-cerebral blood flow and oxygen in humans. Med. Biol. Eng. Comput. 1, 529–536.

Davis, T.L., Kwong, K.K., Weisskoff, R.M., Rosen, B.R., 1998. Calibrated functional MRI: mapping the dynamics of oxidative metabolism. Proc. Natl Acad. Sci. USA 95, 1834–1839.

Dousset, V., Ballarino, L., Delalande, C., Coussemacq, M., Canioni, P., Petry, K.G., Caille, J. M., 1999. Comparison of ultrasmall particles of iron oxide (USPIO)-enhanced T2-weighted, conventional T2-weighted, and gadolinium-enhanced T1-weighted MR images in rats with experimental autoimmune encephalomyelitis. Am. J. Neuroradiol. 20, 223–227.

El-Deab, M.S., Ohsaka, T., 2003. Quasi-reversible two-electron reduction of oxygen at gold electrodes modified with a self-assembled submonolayer of cysteine. Electrochem. Commun. 5, 214–219.

Gilmour, G., Ishiwari, K., Conway, M.W., Lowry, J.P., Tricklebank, M., 2009. Eli Lilly & Co. Ltd., Surrey, UK. Unpublished results.

Gordon, G.R.J., Choi, H.B., Rungta, R.L., Ellis-Davies, G.C.R., MacVicar, B.A., 2008. Brain metabolism dictates the polarity of astrocyte control over arterioles. Nature 456, 745–749.

Hitchman, M.L., 1978. Measurement of dissolved oxygen. John Wiley, New York, USA.

Holmström, N., Nilsson, P., Carlsten, J., Bowald, S., 1998. Long-term in vivo experience of an electrochemical sensor using the potential step technique for measurement of mixed venous oxygen pressure. Biosens. Bioelectron. 13, 1287–1295.

Houston, G.C., Papadakis, N.G., Carpenter, T.A., Hall, L.D., Mukherjee, B., James, M.F., Huang, C.L.-H., 2001. Mapping of brain activation in response to pharmacological agents using fMRI in the rat. Magn. Reson. Imaging 19, 905–919.

Hsia, C.C.W., 1998. Respiratory function of hemoglobin. New Engl. J. Med. 338, 239–248.

Iadecola, C., Nedergaard, M., 2007. Glial regulation of the cerebral microvasculature. Nat. Neurosci. 10, 1369–1376.

Ireland, D., Lowe, A.S., Reavill, C., James, M.F., Leslie, R.A., Williams, S.C.R., 2005. Mapping the effects of the selective dopamine D_2/D_3 receptor agonist quinelorane using pharmacological MRI. Neuroscience 133, 315–326.

Ishiwari, K., Conway, M.W., Gilmour, G., Lowry, J.P., Tricklebank, M., 2009. Acute administration of ketamine increases tissue oxygen levels in the medial prefrontal cortex and the nucleus accumbens shell in freely moving rats. Online Neuroscience Meeting Planner, 443.14. Society for Neuroscience, Washington, DC, USA.

Jones, N., O'Neill, M.J., Tricklebank, M., Libri, V., Williams, S.C.R., 2005. Examining the neural targets of the AMPA receptor potentiator LY404187 in the rat brain using pharmacological magnetic resonance imaging. Psychopharmacology 180, 743–751.

Leontiev, O., Dubowitz, D.J., Buxton, R.B., 2007. $CBF/CMRO_2$ coupling measured with calibrated BOLD fMRI: sources of bias. Neuroimage 36, 1110–1122.

Li, B., Freeman, R.D., 2007. High-resolution neurometabolic coupling in the lateral geniculate nucleus. J. Neurosci. 27, 10223–10229.

Li, J., Gilmour, G., Lowry, J.P., Tricklebank, M., Bannerman, D.M., McHugh, S.B., 2009. Correlations between behavioural responding and amygdala tissue oxygen levels during rat fear conditioning studies. Online Neuroscience Meeting Planner, 192.18. Society for Neuroscience, Washington, DC, USA.

Lowe, A.S., Williams, S.C.R., Symms, M.R., Stolerman, I.P., Shoaib, M., 2002. Functional magnetic resonance neuroimaging of drug dependence: naloxone-precipitated morphine withdrawal. Neuroimage 17, 902–910.

Lowe, A.S., Sloan, H.L., Sibson, N.R., Barker, G.J., 2007. Improved sensitivity to BOLD contrast with multi-echo gradient echo imaging. Proceedings International Society for Magnetic Resonance in Medicine, P. Int. Soc. Magnet. Reson. Med., 4181.

Lowry, J.P., O'Neill, R.D., 1996. Characterisation of carbon paste electrodes *in vitro* for simultaneous amperometric measurement of changes in oxygen and ascorbic acid concentrations *in vivo*. Analyst 121, 761–766.

Lowry, J.P., O'Neill, R.D., 2005. Neuroanalytical chemistry in vivo using biosensors. In: Grimes, C.A., Dickey, E.C. (Eds.), Encyclopedia of Sensors. American Scientific Publishers, Stevenson Ranch, CA, USA, pp. 501–524.

Lowry, J.P., Boutelle, M.G., Fillenz, M., 1997. Measurement of brain tissue oxygen at a carbon paste electrode can serve as an index of increases in regional cerebral blood flow. J. Neurosci. Methods 71, 177–182.

Lowry, J.P., Demestre, M., Fillenz, M., 1998. Relation between cerebral blood flow and extracellular glucose in rat striatum during mild hypoxia and hyperoxia. Dev. Neurosci. 20, 52–58.

Mandeville, J.B., Jenkins, B.G., Chen, Y.C., Choi, J.K., Kim, Y.R., Belen, D., Liu, C., Kosofsky, B.E., Marota, J.J., 2004. Exogenous contrast agent improves sensitivity of gradient-echo functional magnetic resonance imaging at 9.4 T. Magn. Reson. Med. 52, 1272–1281.

Masamoto, K., Omura, T., Takizawa, N., Kobayashi, H., Katura, T., Maki, A., Kawaguchi, H., Tanishita, K., 2003. Biphasic changes in tissue partial pressure of oxygen closely related to localized neural activity in guinea pig auditory cortex. J. Cereb. Blood Flow Metab. 23, 1075–1084.

Masamoto, K., Vazquez, A., Wang, P., Kima, S.-G., 2008. Trial-by-trial relationship between neural activity, oxygen consumption, and blood flow responses. Neuroimage 40, 442–450.

Offenhauser, N., Thomsen, K., Caesar, K., Lauritzen, M., 2005. Activity-induced tissue oxygenation changes in rat cerebellar cortex: interplay of postsynaptic activation and blood flow. J. Physiol. 565, 279–294.

Ogawa, S., Tank, D.W., Menon, R., Ellermann, J.M., Kim, S.G., Merkle, H., 1992. Intrinsic signal changes accompanying sensory stimulation: functional brain mapping with magnetic resonance imaging. Proc. Natl Acad. Sci. USA 89, 5951–5955.

O'Neill, R.D., 1994. Microvoltammetric techniques and sensors for monitoring neurochemical dynamics *in vivo* - a review. Analyst 119, 767–779.

O'Neill, R.D., Lowry, J.P., Mas, M., 1998. Monitoring brain chemistry in vivo: voltammetric techniques, sensors and behavioral applications. Crit. Rev. Neurobiol. 12, 69–127.

Preece, M., Mukherjee, B., Huang, C.L.-H., Hall, L.D., Leslie, R.A., James, M.F., 2001. Detection of pharmacologically mediated changes in cerebral activity by functional magnetic resonance imaging: the effects of sulpiride in the brain of the anaesthetised rat. Brain Res. 916, 107–114.

Raichle, M.E., 1998. Behind the scenes of functional brain imaging: a historical and physiological perspective. Proc. Natl Acad. Sci. USA 95, 765–772.

Seagard, J.L., Bosnjak, Z.J., Hopp Jr., F.A., Kampine, J.P., 1985. Cardiovascular effects of general anesthesia. In: Covino, B.G., Fozzard, H.A., Rehder, K., Strichartz, G. (Eds.), Effects of Anesthesia. Bethesda, American Physiological Society, Bethesda, MD, USA, pp. 149–177.

Stamford, J.A., Justice, J.B., 1996. Probing brain chemistry. Anal. Chem. 68, A359–A363.

Tadamura, E., Hatabu, H., Li, W., Prasad, P.V., Edelman, R.R., 1997. Effect of oxygen inhalation on relaxation times in various tissues. J. Magn. Reson. Imaging 7, 220–225.

Taylor, R.J., Humffray, A.A., 1975. Electrochemical studies on glassy carbon electrodes. 3. Oxygen reduction in solutions of low pH (pH less than 10). J. Electroanal. Chem. Interfacial Electrochem. 64, 85–94.

Thompson, J.K., Peterson, M.R., Freeman, R.D., 2003. Single-neuron activity and tissue oxygenation in the cerebral cortex. Science 299, 1070–1072.

Thompson, J.K., Peterson, M.R., Freeman, R.D., 2004. High-resolution neurometabolic coupling revealed by focal activation of visual neurons. Nat. Neurosci. 7, 919–920.

Thompson, J.K., Peterson, M.R., Freeman, R.D., 2005. Separate spatial scales determine neural activity-dependent changes in tissue oxygen within central visual pathways. J. Neurosci. 25, 9046–9058.

Travis Jr., R.P., Clark Jr., L.C., 1965. Changes in evoked brain oxygen during sensory stimulation and conditioning. Electroencephalogr. Clin. Neurophysiol. 19, 484–491.

Venton, B.J., Michael, D.J., Wightman, R.M., 2003. Correlation of local changes in extracellular oxygen and pH that accompany dopaminergic terminal activity in the rat caudate-putamen. J. Neurochem. 84, 373–381.

Viswanathan, A., Freeman, R.D., 2007. Neurometabolic coupling in cerebral cortex reflects synaptic more than spiking activity. Nat. Neurosci. 10, 1308–1312.

Ward, W.K., Wood, M.D., Slobodzian, E.P., 2002. Continuous amperometric monitoring of subcutaneous oxygen in rabbit by telemetry. J. Med. Eng. Technol. 26, 158–167.

Westerink, B.H.C., Cremers, T., 2007. Handbook of Microdialysis, Volume 16: Methods, Applications and Perspectives. Academic Press, Amsterdam, The Netherlands.

Zhang, Y.N., Wilson, G.S., 1993. In vitro and in vivo evaluation of oxygen effects on a glucose oxidase based implantable glucose sensor. Anal. Chim. Acta 281, 513–520.

Zimmerman, J.B., Wightman, R.M., 1991. Simultaneous electrochemical measurements of oxygen and dopamine in vivo. Anal. Chem. 63, 24–28.